Seasonal climate summary southern hemisphere (spring 2006): a weak El Niño in the tropical Pacific – warm and dry conditions in eastern and southern Australia

Lixin Qi
National Climate Centre, Bureau of Meteorology, Australia

(Manuscript received August 2007)

Southern hemisphere circulation patterns and associated anomalies for the austral spring 2006 are reviewed. Particular emphasis is given to the Australian and Pacific regions. After developing during the winter, spring 2006 saw an El Niño event in the equatorial Pacific Ocean reach its maturity. Ocean surface and subsurface temperatures in the central to eastern tropical Pacific remained well above normal throughout the season, affecting many features of the general circulation and resulting in significant impacts in both the northern and southern hemispheres. For Australia, widespread dry conditions dominated the east and south, consistent with historical El Niño impacts. Many new spring temperature records were also set. Such warm and dry conditions intensified the long-term drought for much of eastern and southern Australia. Over the Antarctic, the size of the ozone hole during spring 2006 was at record or near-record levels.

Introduction

The year 2006 featured a transition, from weak cool (La Niña-like) conditions in the first half of the year, to warm (El Niño-like) conditions in winter (Murphy 2007; Arguez et al. 2007; Mullen and Beard 2006). By the end of August, El Niño conditions were observed across most atmospheric and oceanic indices, and correspondingly, much of Australia had become drier than normal (Murphy 2007). Winter had also brought above average maximum and below average minimum temperatures.

Corresponding author address: Lixin Qi, National Climate Centre, Bureau of Meteorology, GPO Box 1289, Melbourne, Vic. 3001, Australia.
Email: l.qi@bom.gov.au

During the austral spring of 2006, the El Niño – Southern Oscillation (ENSO) intensified and maintained its warm state. The Southern Oscillation Index (SOI) remained negative throughout the season, while sea-surface temperature (SST) anomaly values were positive in the central and eastern equatorial areas. Subsurface values also remained warmer than normal along the equator east of the date-line. Negative anomalies of outgoing long wave radiation (OLR) highlighted the atmospheric response, with increased cloud activity along the equator close to the date-line.

Typically, the maximum extent of the Antarctic ozone hole appears in austral spring. In spring 2005 (Arblaster 2006), the ozone hole was considered the third largest on record, much larger than in spring

2003. For 2006, the Antarctic ozone hole was the largest on record.

This summary reviews the southern hemisphere and equatorial climate patterns for spring 2006, with particular attention given to the Australasian and Pacific regions. The main sources of information for this report are analyses prepared by the Bureau of Meteorology's National Climate Centre, the Bureau's *Monthly Significant Weather Summaries*, the Bureau of Meteorology Research Centre (BMRC), and the *Climate Diagnostics Bulletin* (Climate Prediction Center, Washington).

Pacific Basin climate indices

The Troup South Oscillation Index

The SOI is calculated from the standardised difference between the mean sea-level pressure (MSLP) between Tahiti and Darwin. Figure 1 shows the SOI values from January 2002 to November 2006, together with a five-month weighted moving average. The means and standard deviations used in Fig. 1 are based on the period 1933-1992.

The low SOI values in winter and spring 2006 reflected a sustained warming of the central and eastern tropical Pacific Ocean. The notable negative SOI values in June (−5.5), July (−8.9), August (−15.9), and seasonal mean (−10.1) in winter 2006 (Murphy 2007) were followed by −5.1, −15.3 and −1.4 for September, October and November, respectively, with a resulting seasonal average of −7.3. The negative SOIs were largely the result of above average MSLP at Darwin, while MSLP at Tahiti fluctuated around the average in the first two months. For September, October and November, the MSLP anomalies at Darwin were 1.4, 2.3 and 1.1 hPa, respectively; at Tahiti, the anomalies were 0.3, −0.4 and 1.1 hPa, respectively.

The low SOI values were supported by the Multivariate ENSO Index (MEI) (Wolter and Timlin 1998). The MEI is derived from six atmospheric and oceanic indicators over the tropical Pacific: sea-level pressure, zonal and meridional components of the surface wind, sea-surface temperature, surface air temperature, and total cloudiness fraction of the sky. Positive MEI values of above 0.8 are generally observed during warm ENSO phases (El Niño). The MEI values for August/September, September/October and October/November 2006 were 0.892, 1.027 and 1.293, respectively.

In September, an El Niño event was declared by a number of National Meteorological and Hydrological Services. The El Niño event was the dominant cause of the severe drought experienced throughout south-east Australia in 2006.

Fig. 1 Southern Oscillation Index, from January 2002 to November 2006. Means and standard deviations used in the computation of the SOI are based on the period 1933-1992.

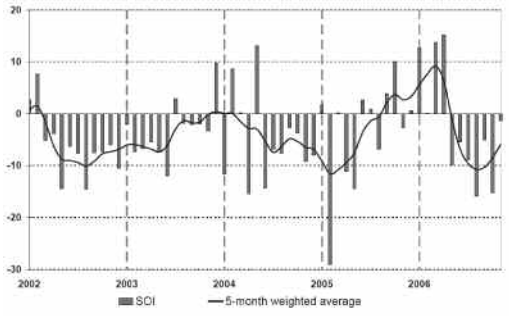

Fig. 2 Standardised anomaly of monthly outgoing long wave radiation averaged over the area 5°S to 5°N and 160°E to 160°W, from January 2002 to November 2006. Negative (positive) anomalies indicate enhanced (reduced) convection and rainfall in the area. Anomalies are based on the 1979-1995 base period. After CPC (2006).

Outgoing long wave radiation (OLR)

Figure 2 displays OLR data from the Climate Prediction Center (CPC, Washington), showing the standardised monthly anomaly from January 2002 to November 2006, together with a three-month moving average. The data are a measure of long wave radiation emitted from an equatorial region centred about the date-line (5°S to 5°N and 160°E to 160°W). Tropical deep convection in this region is particularly sensitive to changes in the phase of the Southern Oscillation. During the warm phase (El Niño) of ENSO, convection is generally more prevalent, resulting in a reduction in OLR. This reduction is due to the lower effective black-body temperature and is associated with increased high cloud and deep convection. The reverse applies in cold (La Niña) events, with less convection expected in the vicinity of the date-line.

The El Niño event in spring 2006 was accompanied by negative OLR anomalies (increased convective activity) along the equator near the date-line. Peak anomaly values were around –0.8 standard deviations. During the individual months of spring 2006, the OLR anomalies for the region were –0.2, –0.8 and –0.2, respectively. By the end of spring, the OLR was clearly showing a rising trend. Normally during a strong El Niño event, there are significant sustained negative OLR values; for example, the OLR values for individual months of spring 2002 were –1.8, –1.3 and –1.4, respectively. The relatively weak negative values in spring 2006 suggest that the 2006 El Niño event was at a weak to moderate level.

Oceanic patterns

Sea-surface temperatures

Figure 3 shows spring 2006 sea-surface temperature (SST) anomalies. These have been obtained from the NOAA Optimum Interpolation analyses (Reynolds et al. 2002). Positive anomalies are shown in pink and red shades, while negative anomalies are shown in blue shades. The contour interval is 0.5°C.

Winter sea-surface temperatures were slightly above average in the central and eastern tropical Pacific (Murphy 2007), but underwent a rapid increase towards the end of the season and into the spring. As a result, the spring SST pattern featured warmer than average temperatures across the central and eastern Pacific, with positive anomalies along the equator from the date-line to South America. NINO 4 (5°S-5°N, 160°E-150°W), NINO 3.4 (5°S-5°N, 170°W-120°W), NINO 3 (5°S-5°N, 150°W-90°W) and NINO1+2 (0°-10°S, 80°W-90°W) were all positive (Table 1). At least two regions (around the date-line and in the eastern Pacific) contained maximum anomaly values exceeding +1.5°C (Fig. 3). Apart from NINO 3.4 in September 2006, all NINO SST values exceeded +0.8 throughout the season (Table 1).

Table 1. SST anomalies in NINO regions during spring 2006. The base period to calculate the anomalies is from 1971 to 2000.

	NINO 1+2	*NINO 3*	*NINO 4*	*NINO3.4*
September 2006	0.94	0.91	0.92	0.70
October 2006	1.31	1.07	1.03	0.88
November 2006	1.04	1.12	1.26	1.21

In the Indian Ocean, the Indian Ocean Dipole strengthened further from its winter pattern, characterised by a significant cooling of SSTs southwest of Indonesia, and the development of warm SST anomalies in the western Indian Ocean. Coastal waters off the northwest of Western Australia were slightly warmer than average.

Subsurface patterns

Figure 4 shows the time evolution of anomalies in the depth of the 20°C isotherm along the equator from August 2001 to November 2006. The 20°C isotherm depth is generally close to the equatorial ocean thermocline, the region of greatest temperature gradient with depth and the boundary between the warm near-surface and cold deep-ocean waters. Positive anomalies correspond to the 20°C isotherm being deeper than average, and negative anomalies to it being shallower than average. Changes in the thermocline depth can be an indicator for subsequent changes at the surface.

Fig. 3 Anomalies of sea-surface temperature for spring 2006 (°C). The contour interval is 0.5°C.

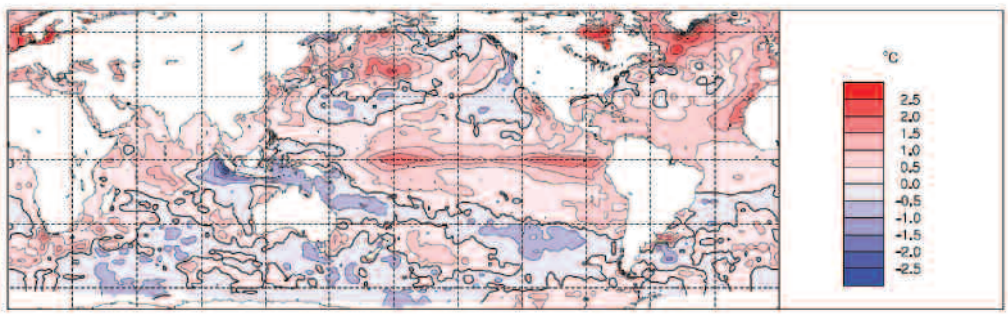

Fig. 4 **Time-longitude section of the monthly anomalous depth of the 20°C isotherm at the equator from January 2001 to November 2006. The contour interval is 10 m.**

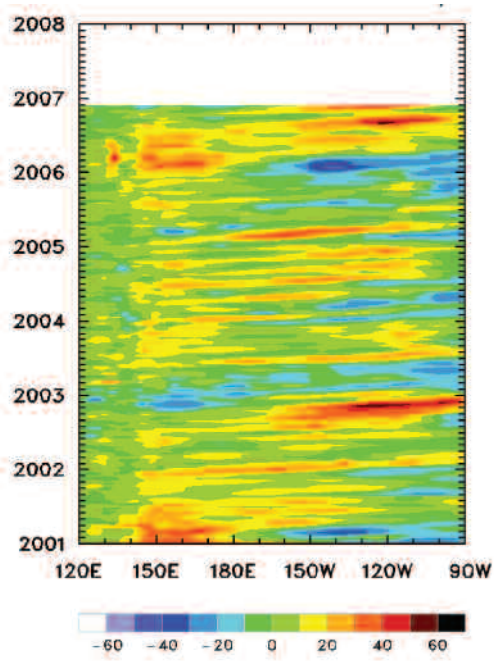

In the western Pacific basin, westerly wind bursts were observed at the surface during each individual spring month (not shown here). As a result of this significant weakening of the easterly Trade Winds, eastward-propagating oceanic Kelvin waves were generated, resulting in a maximum anomaly value for isotherm depth at around 120°W in November. Correspondingly, subsurface temperatures were close to or slightly lower than average in the western and central Pacific.

Figure 5 shows a cross-section of equatorial subsurface temperature anomalies from August to November 2006, down to 400 metres. Red shades indicate positive anomalies, and blue shades negative anomalies. Throughout the season, positive anomalies were present in the central and eastern Pacific to a depth of approximately 200 m, peaking in November around 135°W, with a maximum anomaly of 4°C. West of the dateline, negative anomalies around the depth of 150 m were more intense in September and November than in October. Compared with August, the maximum areas of positive anomalies in spring were closer to the surface, and the intensity in November was significantly stronger than that in August.

Fig. 5 **Four-month August to November 2006 sequence of vertical temperature anomalies at the equator for the Pacific Ocean. The contour interval is 0.5°C.**

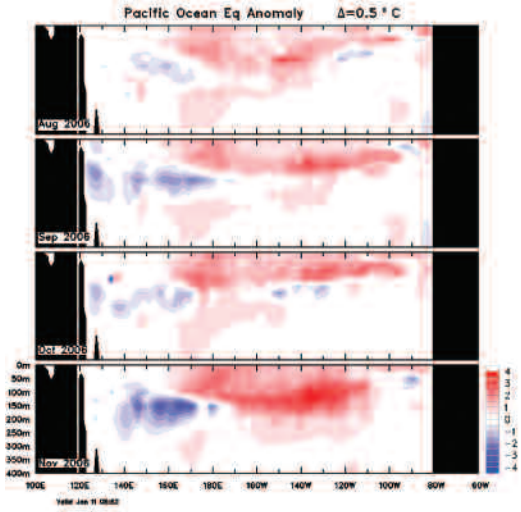

The subsurface anomalies throughout the equatorial Pacific were generally within the range −3°C to +4°C. The area covered by +4°C was bigger than that which occurred during spring 2004, a neutral year with neutral to weakly warm subsurface conditions (Watkins 2005). Considering the peak of the El Niño event in 1997-98 saw subsurface anomalies reach in excess of +8°C, spring 2006 can be classified as weakly warm in the subsurface.

By September it was clear that the warm SST anomalies would be sustained, and hence an El Niño event was declared by a number of National Meteorological and Hydrological Services.

Atmospheric patterns

Surface analyses

The spring 2006 MSLP field, calculated from the Bureau of Meteorology's Global Assimilation and Prediction (GASP) model, is shown in Fig. 6, with the associated anomaly pattern in Fig. 7. These anomalies are the difference from a 1979-2000 climatology, obtained from the National Centers for Environmental Prediction (NCEP) II Reanalysis data (Kanamitsu et al. 2002). The MSLP analysis has been computed using data from the 0000 UTC daily analyses of the GASP model. The MSLP anomaly field is not shown over areas of elevated topography (grey shading).

Fig. 6 Spring 2006 mean sea-level pressure (hPa). The contour interval is 5 hPa.

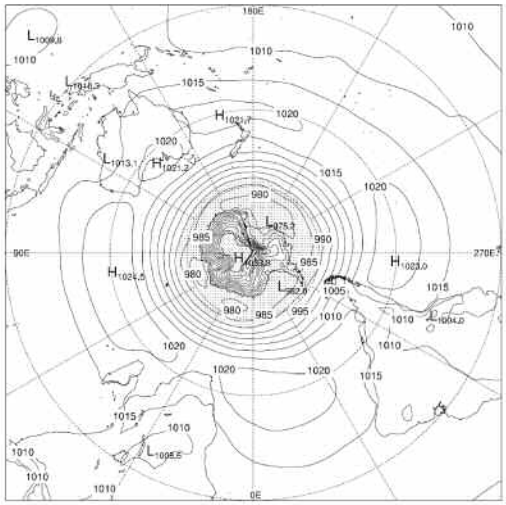

Fig. 7 Spring 2006 mean sea-level pressure anomaly (hPa). The contour interval is 2.5 hPa.

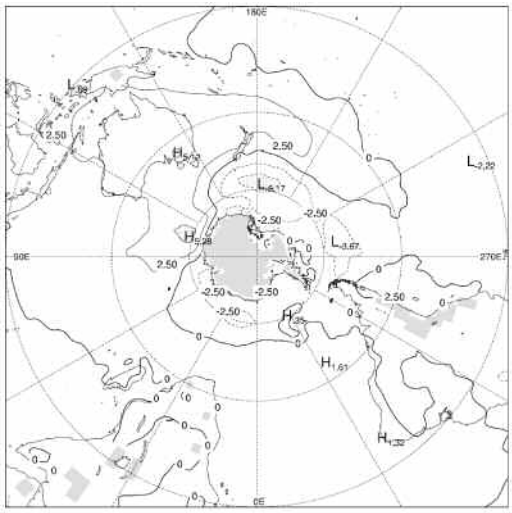

The spring MSLP pattern (Fig. 6) displays a zonal structure with weak wave-three characteristics around Antarctica. The Antarctic circumpolar trough showed three areas where the MSLP was below 980 hPa: 20°E, 70°E, and 180°E to 120°W. Over Australia, the subtropical ridge was located around 30°S. In the anomaly pattern (Fig. 7), high latitude negative anomalies were centred around 170°W (−6.2 hPa) and 100°W (−3.7 hPa), with another main feature being a positive anomaly (central pressure +5.28 hPa) around 110°E.

Most of the MSLP fields over Australia and New Zealand were slightly above average, with the anomalies peaking at +5.1 hPa near Mildura (Victoria). In the tropical Pacific, responding to the warm SST anomalies (Fig. 3), anomalies were mostly negative, but small in magnitude (minimum value: −2.2 hPa). During the 2002 El Niño event, values were as low as −3.9 hPa. This would again suggest that the 2006 El Niño was a relatively weak event.

Mid-tropospheric and blocking analyses

The 500 hPa geopotential height, an indicator of the steering of surface synoptic systems, is shown in Fig. 8, with associated anomalies in Fig. 9. The polar three-wave pattern on the MSLP field also can be seen in Fig. 8. Similarly to the surface, a minimum was located south of New Zealand at around 180°E, 60°S, with a minimum value of −87.6 gpm (Fig. 9), while to the north, over the southwest Indian Ocean, Australia and southern Pacific Ocean, the mid-level heights were above average with a maximum value of 62.8 gpm located off the coastline of South Australia.

The time-longitude section of the daily southern hemisphere Blocking Index (BI)* is shown in Fig. 10, with the start of the season at the top of the diagram. This index is a measure of the strength of the zonal 500 hPa flow in the mid-latitudes (40°S to 50°S) relative to that at subtropical (25°S to 30°S) and high (55°S to 60°S) latitudes. Positive values of the BI are generally associated with a split in the mid-latitude westerly flow centred near 45°S and mid-latitude blocking activity.

Several strong blocking episodes were observed during spring 2006. Blocking was observed from 100°E to 90°W for the first week of September. The second event was centred on the date-line, and started in the first week of October, though was small in comparison with the initial event. Centred around 150°W, another small but strong blocking event occurred in the first week of November. Averaged over the whole season (Fig. 11), blocking was below average for most longitudes, with two notable exceptions where stronger than average blocking occurred; the regions from 90°E to 120°E and from 150°W to 90°W. The peak BI values were located around 140°W.

*The Blocking Index is defined as BI = 0.5 $[(u_{25} + u_{30}) - (u_{40} + 2u_{45} + u_{50}) + (u_{55} + u_{60})]$, where u_x is the westerly component of the 500 hPa wind at latitude x.

Fig. 8 Spring 2006 500 hPa mean geopotential height (gpm). The contour interval is 100 gpm.

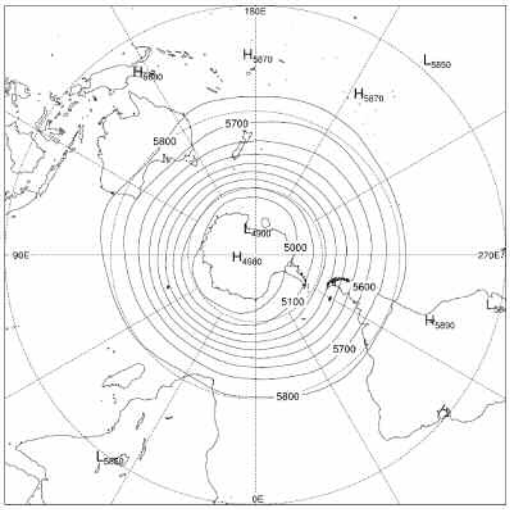

Fig. 9 Spring 2006 500 hPa mean geopotential height anomaly (gpm). The contour interval is 30 gpm.

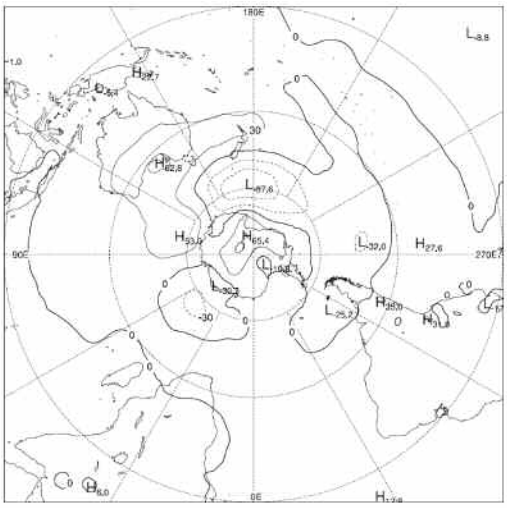

Winds

The low-level (850 hPa) and upper-level (200 hPa) wind anomalies from the 22-year NCEP II climatology for spring 2006 are shown in Fig. 12 and Fig. 13, respectively. Isotach contours are at 5 m s^{-1} intervals, and the regions where the surface rises above 850 hPa are shaded grey in Fig. 13.

Fig. 10 Spring 2006 daily blocking index (m s^{-1}) time-longitude section. The horizontal axis measures degrees of longitude east of the Greenwich meridian. Day one is 1 September.

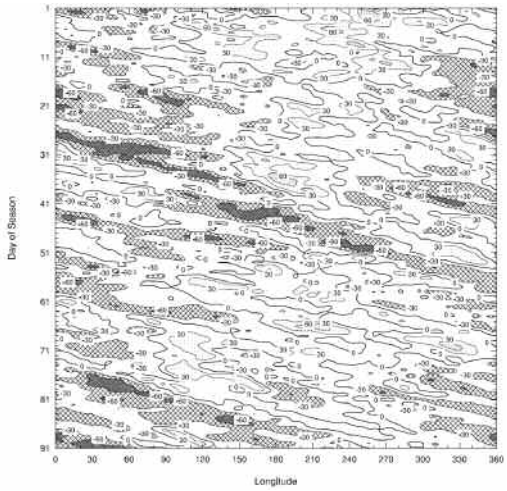

Fig. 11 Mean southern hemisphere blocking index (m s^{-1}) for spring 2006 (solid line). The dashed line shows the corresponding long-term average. The horizontal axis shows degrees east of the Greenwich meridian.

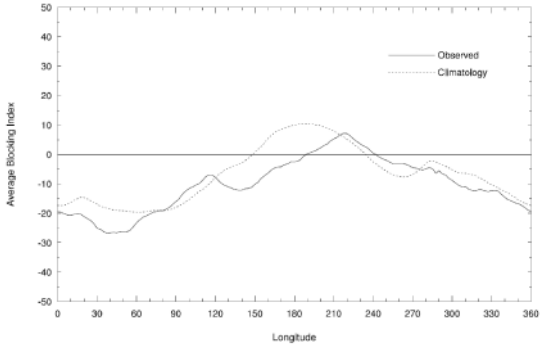

At the 850 hPa level, the wind anomalies generally reflected the MSLP anomalies (Fig. 7). Largest anomalies occurred in the eastern (4.62 m s^{-1}) and western equatorial Pacific Ocean (5.25 m s^{-1}). This pattern indicated a strong suppression of the trade winds, which assisted the development of positive SST anomalies across most of the tropical and equatorial Pacific (Fig. 3), leading to a fully coupled El Niño event.

Fig. 12 Spring 2006 850 hPa vector wind anomalies (m s^{-1}).

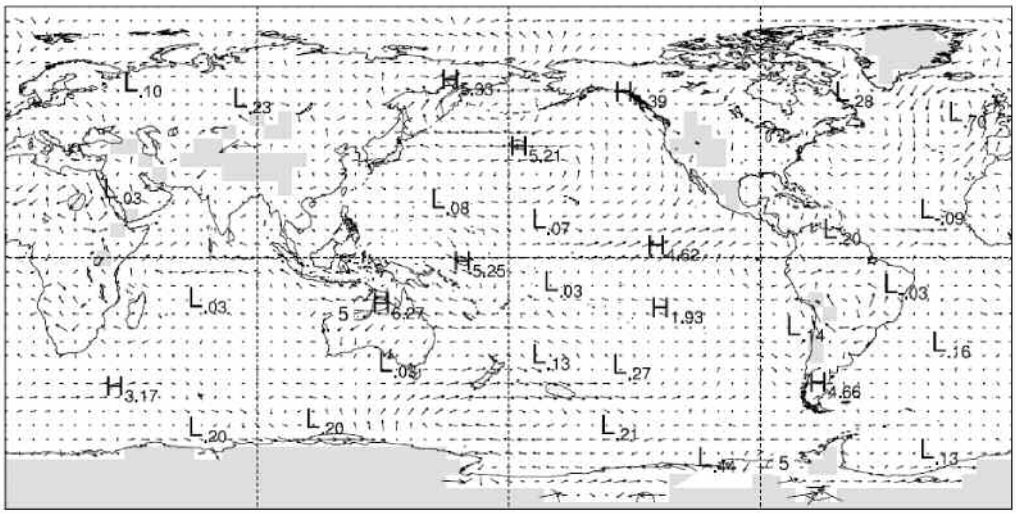

Fig. 13 Spring 2006 200 hPa vector wind anomalies (m s^{-1}).

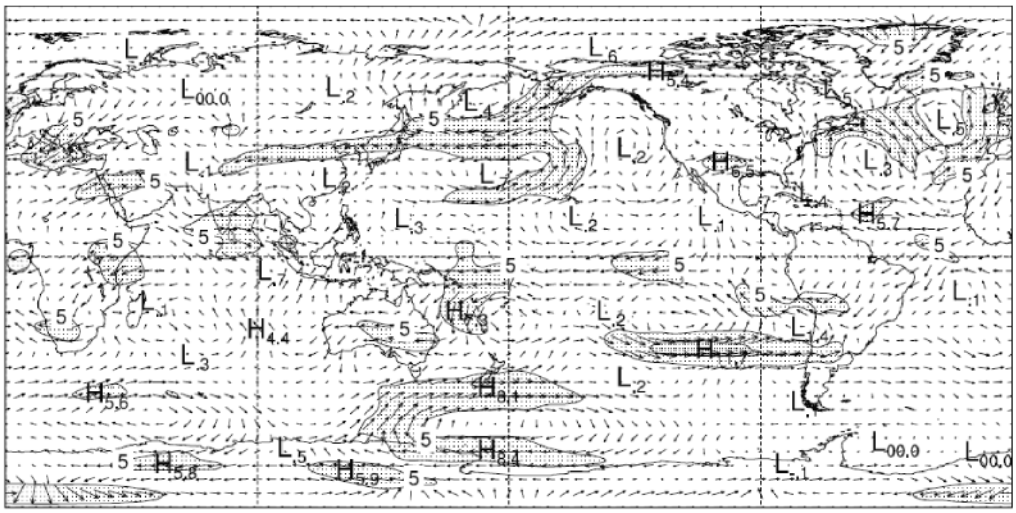

The largest anomalies (6.27 m s^{-1}) occurred over the northern Australian region. A cyclonic anomaly pattern south of New Zealand was prominent, and to a lesser extent the anticyclonic anomaly pattern over the Tasman Sea. Over most of the Indian Ocean, the low-level winds were near average, except for the southwest where the anomalies reached a maximum value of 3.17 m s^{-1}.

At the 200 hPa level (Fig. 13), over the tropical and central equatorial Pacific, both sides of the equator showed anticyclonic anomaly patterns, leading to the area being dominated by easterly anomalies with maximum values above 5 m s^{-1}. Such a pattern is indicative of the breakdown of the Walker Circulation, and hence the development of an El Niño event. At higher latitudes, cyclonic patterns were dominant south of New Zealand and south of Madagascar.

Ozone hole observations

Typically, the austral spring is the time of the maximum extent of the Antarctic ozone hole, together with the lowest annual ozone levels. In the absence of sunlight, the wintertime polar vortex in the lower stratosphere cools to below –78°C, enabling polar stratospheric ice clouds to form. Chlorine and bromine compounds react in the ice clouds to produce chemical species that, when combined with the incoming UV radiation as the sunlight returns in spring, destroy ozone. As the stratosphere warms in spring (and hence ice clouds can no longer form) this process weakens. Ozone levels then return to near normal by early summer.

Spring ozone totals are shown in Fig. 14, taken from the Total Ozone Mapping Spectrometer (TOMS) and Ozone Monitoring Instrument (OMI) (http://toms.gsfc.nasa.gov). Ozone values are given in Dobson Units and the ozone hole is typically taken as the region where values of total column ozone are less than 220 Dobson units.

The size of the south polar vortex was notably large in spring 2006. On 1 October, the vortex area at 70 hPa was 34 million km^2, the largest such area observed for this date since vortex size records commenced in 1986. Minimum temperatures at 50 hPa in the vortex south of 50°S dropped to their lowest levels since records commenced in 1979. On 25 September, the ozone hole area, as measured by TOMS and OMI, reached a peak of 29.5 million km^2, breaking the previous record of 29.4 million km^2 observed in September 2000, whilst other instruments also showed record or near-record ozone hole size (WMO 2006). Observations from the Global Ozone Monitoring Experiment (GOME) and the Scanning Imaging Absorption Spectrometer for Atmospheric Chartography (SCIAMACHY) suggest the ozone mass deficit reached a record high value of 40.8 megatonnes in early October.

Fig. 14 Total column ozone values from the Ozone Monitoring Instrument (OMI) for spring 2006 (Dobson Units).

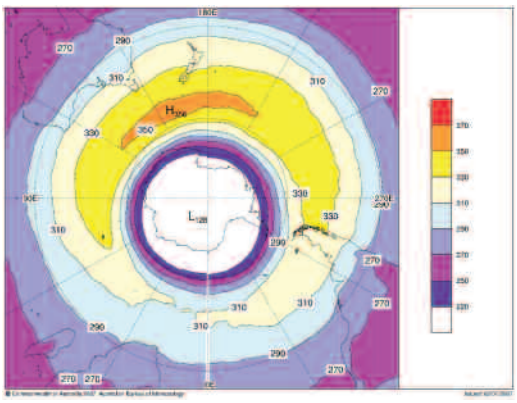

The unusually large ozone hole area and the high ozone mass deficit were caused by the extremely cold temperatures in the Antarctic region coupled with an anomalously large polar vortex, resulting in abundant ozone-depleting substances in the stratosphere and thus severe ozone destruction.

Recent years have shown much variability in the size of the Antarctic ozone hole. In spring 2004 the ozone hole was relatively small (Watkins 2005), whereas in 2005 it was much larger (Arblaster 2006), before the record size observed in 2006. The interannual variation of the ozone hole is consistent with the existing level of ozone-depleting substances in the atmosphere (Arguez et al. 2007), despite some recent decrease in such substances resulting from the Montreal Protocol. The decrease of ozone-depleting substances is expected to take decades to show its effects. The ozone hole is not expected to commence shrinking until at least 2010, and may disappear by 2070 (Newman et al. 2006).

Australian region

Rainfall

Figure 15 shows the spring rainfall totals for Australia, while Fig. 16 shows the spring rainfall deciles, where the deciles are calculated with respect to gridded rainfall data for all springs from 1900 to 2006.

The highest rainfall totals during spring 2006 were along the central New South Wales coast and the area south of Cairns in Queensland. However, in general the impacts of the positive MSLP anomalies (Fig. 7) and negative SOI (Fig. 1) on rainfall were clearly evident, with spring rainfall below to very much below average across most of the eastern half of the country. Lowest on record totals were observed over parts of Victoria, New South Wales, Northern Territory and South Australia. A broad region across Northern Territory, Queensland, New South Wales and South Australia recorded below to very much below average rainfall. In sharp contrast, central and northwest Western Australia experienced above to very much above average rainfall. The area to the southeast of Port Hedland recorded their highest spring totals on record.

In terms of the monthly outcomes, September rainfall was below to very much below average across much of the country away from the east coast except for the northwest of Western Australia. In October the very dry conditions extended from South Australia to

Victoria, New South Wales, Queensland and northern Tasmania, with many areas with lowest on record monthly rainfall across the east and south. November rainfall was relatively close to the average.

In area-averaged terms, rainfalls are ranked from the lowest to highest in Table 2. Spring 2006 was nationally ranked 16th driest out of 107 years (1900 to 2006) of record. Victoria and South Australia experienced their third lowest spring rainfall on record, while heavy rains in central and northwest Western Australia contributed to a statewide average in Western Australia which ranked 91 of 107, the highest since 2001.

During El Niño events, most areas of southern and eastern Australia expect below-average rainfall. As in spring 2002, the rainfall pattern in spring 2006 was consistent with typical El Niño impacts upon Australia. The low rainfalls during spring 2006 further compounded the long-term drought in southern and eastern Australia, which in many areas had seen little recovery from severe El Niño-related dry conditions of 2002-03 and in some locations 1997-98.

Over the last 50 years, there has been a substantial decline in rainfall over much of southern and eastern Australia, with offsetting increases in the northwest (Bureau of Meteorology 2007). Many other countries also have had severe dry conditions, and the area affected by severe drought increased from approximately 10%-15% of the world's land area in the 1970s to 30% in 2002 (Arguez et al. 2007). Zhang et al. (2007) examined human-induced impacts on global precipitation, suggesting that there has been a detectable anthropogenic influence on rainfall in the northern hemisphere and parts of the southern hemisphere. Further investigation is needed in order to identify the possible regional impacts in Australia.

Fig. 15 Spring 2006 rainfall totals (mm) in Australia.

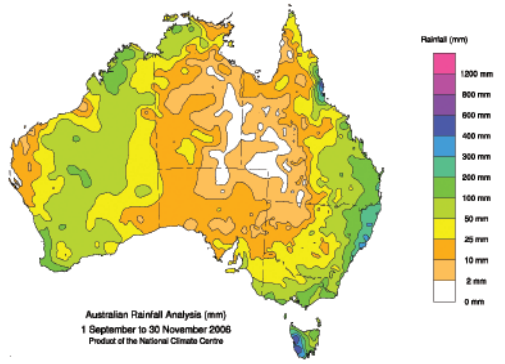

Fig. 16 Spring 2006 rainfall for Australia: decile range values based on grid-point values over the springs 1900 to 2006.

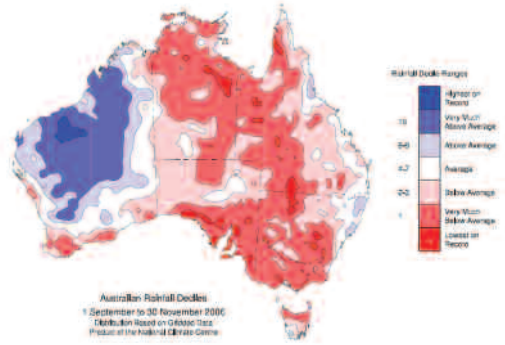

Temperatures

Figures 17 and 18 show the mean Australian maximum and minimum temperature anomalies for spring 2006. The anomalies have been calculated with respect to the standard 1961-1990 reference period. A high-quality subset of the network is used to calculate the spatial averages and rankings shown in Tables 3 and 4, using data from 1950 to the present. All ranking of spring 2006 temperatures against the historical record is done in terms of this high-quality subset.

Seasonal maximum temperatures (Fig. 17) were above average across most of the country, the most notable exception being across northeast Queensland, small parts of the Northern Territory, northern Western Australia and the western coastline of Tasmania. In area-averaged terms (Table 3) spring 2006 was nationally the warmest on record, with a maximum temperature anomaly of +1.82°C with respect to the 1950 to 2006 period. For individual States and Territories, Victoria, South Australia and Western Australia also experienced their warmest spring on record; New South Wales and Northern Territory reached their second highest and third highest, respectively, and Queensland and Tasmania also had positive anomalies. As in winter 2006 (Murphy 2007), maximum temperatures were generally above average in the south and below average in the north; however, the areas which were below average were much smaller in spring. The largest positive anomaly was recorded in the area north of Canberra, with anomaly values above +4°C, and the lowest in the Normanton (far north Queensland) area, with some values below -1°C. On 30 November, Australia's highest daily maximum temperature in spring 2006 (48.5°C) was recorded at Birdsville Airport in Queensland, which is also the highest temperature in 2006 and the second-highest November temperature on record for Australia.

Table 2. Seasonal rainfall ranks and extremes on a national and State basis for spring 2006.

	Highest seasonal total (mm)	*Lowest seasonal total (mm)*	*Highest 24-hour fall (mm)*	*Area-averaged rainfall (AAR) (mm)*	*Rank of AAR**
Australia	1378 at Bellenden Ker Top Station (QLD)	Zero at several locations	295 at Trebonne Al, 3 September (QLD)	43.6	16
WA	223 at Huntly	Zero at several locations	83 at Sturt Creek, 27 October	56.7	91
NT	264 at Middle Point	Zero at several locations	112 at Middle Point, 5 November	19.1	5
SA	128 at Woodhouse	Zero at several locations	33 at Leaward, 12 November	15.6	3
QLD	1378 at Bellenden Ker Top Station	Zero at several locations	295 at Trebonne Al, 3 September	37.5	10
NSW	515 at Smiths Lake	Zero at several locations	160 at Smiths Lake, 5 November	67.4	14
VIC	334 at Mt Baw Baw	14 at Gama	58 at Orbost, 9 September	72.5	3
TAS	815 at Strathgordon	51 at Bell Bay	42 at Mt Read, 24 September	225.7	17

* The rank goes from 1 (lowest) to 107 (highest) and is calculated for the years 1900 to 2006 inclusive.

Table 3. Seasonal maximum temperature ranks and extremes on a national and State basis for spring 2006.

	Highest seasonal mean (°C)	*Lowest seasonal mean (°C)*	*Highest daily recording (°C)*	*Lowest daily recording (°C)*	*Anomaly of area-averaged mean (°C) (AAM)*	*Rank of AAM**
Australia	39.7 at Fitzroy Crossing (WA)	7.4 at Mt Read (TAS)	48.5 at Birdsville Airport (QLD), 30 November	–3.0 at Mt Hotham (VIC), 15 November	+1.82	57
WA	39.7 at Fitzroy Crossing	19.3 at North Walpole	46.4 at Emu Creek, 22 November	10.5 at Rocky Gully, 4 September	+1.88	57
NT	38.4 at Bradshaw	30.8 at Gove	45.3 at Jervois, 30 November	18.4 at Arltunga, 10 September	+1.51	55
SA	33.1 at Oodnadatta	16.6 at Mt Lofty	47.3 at Oodnadatta Airport, 29 November	6.5 at Mt Lofty, 6 & 24 September	+2.67	57
QLD	37.1 at Century Mine	23.1 at Applethorpe	48.5 at Birdsville Airport, 30 November	11.4 at Applethorpe, 7 September	+0.93	49
NSW	31.5 at Mungindi	10.1 at Thredbo Top Station	44.3 at White Cliffs, 28 November	–1.8 at Thredbo Top Station, 15 November	+2.95	56
VIC	26.3 at Mildura	9.6 at Mt Hotham	41.4 at Hopetoun, 21 November	–3.0 at Mt Hotham, 15 November	+2.31	57
TAS	18.6 at Campania	7.4 at Mt Read	34.3 at Campania, 12 October	–1.3 at Mt Wellington, 15 November	+0.36	38

* The temperature ranks go from 1 (lowest) to 57 (highest) and are calculated for the years 1950 to 2006 inclusive.

Seasonal minimum temperatures (Fig. 18) were generally above average across most central latitudes of the country, where temperatures were between 1°C and 3°C above average. In contrast, much of Victoria, Tasmania, the central and northern areas of Queensland/Northern Territory and northern Western Australia experienced temperatures between 1°C and 2°C below average, exceeding 2°C in a small area. Consistent with the maximum temperature, the minimum temperature for the country was the third highest positive anomaly on

Fig. 17 Spring 2006 maximum temperature anomalies for Australia based on a 1961-1990 mean (°C).

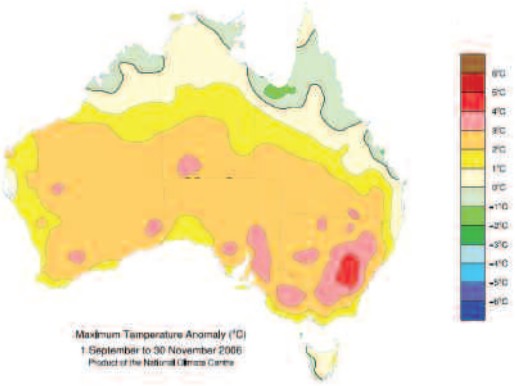

Fig. 18 Spring 2006 minimum temperature anomalies for Australia based on a 1961-1990 mean (°C).

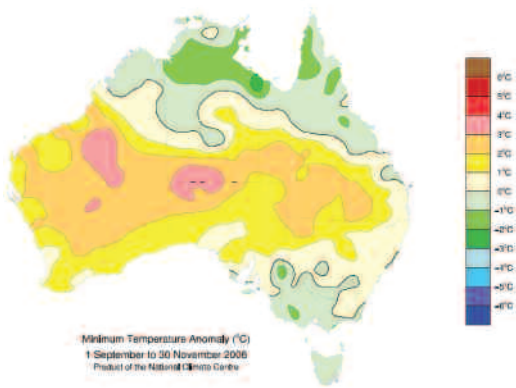

record (Table 4), with Western Australia recording its highest spring minimum temperature since records began with an anomaly of +1.70°C. On the contrary, Victoria and Tasmania were below average. The largest positive anomalies were recorded in central Western Australia and the western border between Northern Territory and South Australia, with values above 3°C, and were lowest in a small area around the northern border between Queensland and Northern Territory, with values around –2°C. On 29 October, Australia's lowest daily minimum temperature in spring 2006 (–12.0°C) was recorded at Charlotte Pass in New South Wales, an Australian record for October.

As for spring 2002 (Watkins 2003), the spatial distributions of the maximum and minimum temperature anomalies were broadly consistent with typical El Niño impacts. However, compared with spring 2002, areas with anomalies above +2°C were more extensive in 2006. The area covered by positive anomalies in the minimum temperature field for spring 2006 was also much larger than that observed in 2002, in particular over central Western Australia and the western border between South Australia and Northern Territory, where maximum anomaly values were above +3°C.

In terms of the mean temperature (not shown),

Table 4. Seasonal minimum temperature ranks and extremes on a national and State basis for spring 2006.

	Highest seasonal mean (°C)	*Lowest seasonal mean (°C)*	*Highest daily recording (°C)*	*Lowest daily recording (°C)*	*Anomaly of area-averaged mean (°C) (AAM)*	*Rank of AAM**
Australia	26.0 at Troughton Island (NT)	–0.3 at Mt Wellington (TAS)	32.6 at Thargomindah (QLD), 28 November	–12.0 at Charlotte Pass (NSW), 29 October	+1.03	55
WA	26.0 at Troughton Island	8.2 at Wandering	32.1 at Telfer, 24 November	–2.2 at Eyre, 14 September	+1.70	57
NT	24.5 at Warruwi	15.5 at Territory Grape Farm	30.2 at Watarrka, 25 November	2.3 at Kulgera, 10 September	+0.54	39
SA	16.9 at Oodnadatta Airport	6.4 at Keith	32.2 at Oodnadatta Airport, 30 November	–3.3 at Keith, 21 October	+1.52	56
QLD	24.0 at Horn Island	9.2 at Applethorpe	32.6 at Thargomindah, 28 November	–0.7 at Stanthorpe, 9 September	+0.54	43
NSW	16.5 at Cape Byron	0.9 at Thredbo Top Station	30.4 at Tibooburra, 28 November	–12.0 at Charlotte Pass, 29 October	+0.79	47
VIC	10.7 at Wilsons Promontory	1.5 at Mt Hotham	24.2 at Walpeup, 21 November	–9.2 at Mt Hotham, 25 September	–0.66	10
TAS	9.8 at Swan Island	–0.3 at Mt Wellington	19.2 at Strahan, 12 October	–7.9 at Liawenee, 16 October	–0.41	20

* The temperature ranks go from 1 (lowest) to 57 (highest) and are calculated for the years 1950 to 2006 inclusive.

with the exception of Tasmania, all the other States and Territory experienced positive anomalies. When averaged across the whole country, Australia recorded its warmest spring on record, with a mean temperature anomaly of +1.42°C.

The dry and warm conditions provided favourable conditions for bushfires, with fires reported in most States. In Victoria, where the bushfire season is generally from November to April, bushfires started as early as the middle of September. For most of southern Australia the bushfire season started unseasonably early during spring 2006.

Acknowledgments

The author would like to thank Robert Fawcett and Grant Beard for their valuable inputs. Andrew Watkins and Blair Trewin provided generous help and excellent comments. A portion of this study is supported by the Australian Greenhouse Office as part of its Bilateral Climate Change Partnerships Programme.

References

Arblaster, J.M. 2006. Seasonal climate summary southern hemisphere (spring 2005): a wet and warm season across much of Australia. *Aust. Met. Mag., 55*, 231-44.

Arguez, A. and 158 others 2007. State of the Climate in 2006, Special Supplement, *Bull. Am. Met. Soc., 88,* 135 pp.

Bureau of Meteorology 2007. *Annual Climate Summary 2006*. National Climate Centre, Bureau of Meteorology, Australia, 16 pp.

Climate Prediction Center 2006. *Climate Diagnostics Bulletin,* Climate Prediction Center, National Weather Service, Washington D.C., USA.

Kanamitsu, M., Ebisuzaki, W., Woollen, J., Yang, S.-K., Hnilo, J.J., Fiorino, M. and Potter, G.L. 2002. NCEP-DOE AMIP-II Reanalysis (R-2). *Bull. Am. Met. Soc., 83*, 1631-43.

Mullen, C. and Beard, G.S. 2006. Seasonal climate summary southern hemisphere (summer 2005-06): a neutral ENSO state with strong climate contrasts across Australia. *Aus. Met. Mag., 55*, 301-12.

Murphy, B.F. 2007. Seasonal climate summary southern hemisphere (winter 2006): El Niño develops late but drought already severe. *Aust. Met. Mag., 56,* 111-21.

Newman, P.A., Nash, E.R., Kawa, S.R., Montzka, S.A. and Schauffler, S.M. 2006. When will the ozone hole recover? *Geophys. Res. Lett., 33,* L12814, doi:10.1029/2005GL025232.

Reynolds, R.W., Rayner, N.A., Smith, T.M., Stokes, D.C. and Wang, W. 2002. An improved in situ and satellite SST analysis for climate. *Jnl Climate, 15*, 1609-25.

Watkins, A.B. 2003. Seasonal climate summary: Southern Hemisphere (spring 2002): the El Niño reaches maturity and dry conditions dominate Australia. *Aust. Met. Mag., 52,* 213-26.

Watkins, A.B. 2005. Seasonal climate summary: Southern Hemisphere (spring 2005): neutral conditions remain in the tropical Pacific and a warm spring across Australia. *Aust. Met. Mag., 54*, 225-39.

Wolter, K. and Timlin, M.S. 1998. Measuring the strength of ENSO – how does 1997/98 rank? *Weather, 53*, 315-24.

World Meteorological Organization (WMO) 2006. *Antarctic Ozone Bulletin, 5*, 2006.

Zhang, X., Zwiers, F.W., Stott, P.A. and Nozawa, T. 2007. Detection of human precipitation trends. *Nature, 448*, 461-5.